10.1109/ULTSYM.2011.0472

Optical Characterization of Individual Liposome-loaded Microbubbles

Ying Luan[1], Telli Faez[1] , Ilya Skachkov[1], Erik Gelderblom[2], Bart Geers[3], Ine Lentacker[3], Ton van der Steen[1], Michel Versluis[2], Nico de Jong[1,2]
[1]Erasmus Medical Center, Rotterdam, the Netherlands
[2]University of Twente, Enschede, the Netherlands
[3]University of Ghent, Ghent, Belgium

Abstract — **Newly developed liposome-loaded (LPS) microbubbles are characterized by comparing their oscillating response with standard phospholipid-coated (bare) microbubbles using the ultra-high speed imaging (Brandaris 128) camera. A study of the shell properties indicate nearly the same shell elasticity and a higher shell viscosity for LPS bubbles than for bare bubbles. A frequency and pressure-dependent bubble acoustical behavior study shows a higher threshold for the initiation of bubble vibrations for LPS bubbles. In addition, an "expansion-only" behavior was observed for up to 69% of the investigated LPS bubbles which mostly occurred at lower acoustic pressures (≤30 kPa). Liposome attachment stability were studied using fluorescence imaging. The internal relationship among morphological structure, shell properties and ultrasonic behavior of LPS bubbles by optical characterization facilitate preclinical study and clinical application of LPS bubbles in ultrasound triggered drug delivery system.**

Keywords – liposome-loaded microbubbles, shell properties, drug delivery

I. INTRODUCTION

The applications of ultrasound-triggered drug delivery system and their underlying physical mechanisms are under extensive investigations nowadays due to their enormous clinical potential in oncology and cardiovascular applications [1]. It has been shown that contrast agent microbubbles are capable of greatly enhancing drug delivery efficiency under ultrasound treatment when applied as a drug delivery vehicle [2]. Instead of previous coadministration of drug molecules and microbubbles, drug loaded microbubbles are developed, to achieve highly efficient and well-controlled drug delivery, under the application of ultrasound radiation.

The liposome-loaded (LPS) microbubble, with drug carrying liposomes attached to the microbubble shell, is a newly developed drug delivery vehicle. Since liposomes are composed of an aqueous core entrapped by lipid bilayers, it is investigated as functional micro-particulate drug carriers for both hydrophobic and hydrophilic drugs. LPS bubbles were firstly developed by Kheirolomoom et al. [3]. Geers *et al*. further modified the formulation by binding liposomes to microbubbles through covalent thoil-maleimide linkages through a single step self-assembly process [4].

Series of physical characterizations performed on LPS bubbles through flow cytometry, coulter counter measurement and confocal fluorescence imaging indicate the concentration, size distribution, and liposome loading amount [4]. However, acoustical characteristic of LPS bubbles, which is essential for further understanding of mechanisms of drug delivery, remains to be incomplete. On the other hand, extensive work has been performed in recent years on the acoustical characterizations of lipid-shelled (bare) microbubbles, both theoretically and experimentally [5-7]. Van der Meer *et al.* [8] estimated the shell properties of BR14 microbubbles by performing microbubble spectroscopy, an optical characterization technique using an ultrahigh-speed camera. Later on, Emmer *et al.* [9] reported the existence of a pressure threshold of bubble oscillation, termed "thresholding" behavior and De Jong *et al*. [10] observed a "compression only" behavior which indicates asymmetrical oscillations of bubbles. These acoustical responses were studied and explained by mathematical models [5-6, 11].

In this study, shell properties as well as the ultrasonic behavior of LPS bubbles as a function of transmit frequencies and acoustical pressures were investigated based on optical approaches. We analyzed the response of insonified single LPS bubbles, by comparing the data recorded with the ultra-high speed Brandaris 128 camera to simulation results obtained from a linearized Marmottant model. The results are then compared with the response of bare bubbles. Furthermore, with the help of fluorescence imaging the stability of liposome attachment on the microbubble shell has been studied.

II. MATERIALS AND METHODS

A. Liposome-loaded microbubbles

Preparation of microbubble samples started from transparent lipid solution or lipid/liposome mixture, in case of bare bubbles and LPS bubbles, respectively, contained in 2.5 ml chromatography vials, with perfluorobutane (C_4F_{10}) filled in the headspace, as was elaborated by Geers *et al.* [4] . Before experiments, microbubbles were obtained in a self-assembly process by high-speed shaking using the Vialmix^{TM} activator (Bristol-Myers Squibb Medical Imaging, North Billerica, MA, USA) at room temperature.

Coulter counter measurements indicate a volume-averaged diameter of 3.6 μm and a concentration of 1.2×10^9 bubbles/ml for bare bubbles. In the case of LPS bubbles, the average diameter and concentration is 4.0 μm and 1.04×10^9 bubbles/ml, respectively. A liposome layer with 600 to 1300 liposomes loaded on the microbubble surface was formed.

B. *Spectroscopy of frequency sweeping experiment*

Fig. 1 shows a schematic view of the experimental setup. An acoustically transparent cellulose capillary tube (Product No. 132294 Spectrum Europe, Breda, NL) was fixed in a water tank and submerged in water. A broadband transducer (PA 086, 0.5-4 MHz, Precision Acoustics, Dorchester, UK) was mounted in the water tank and was focused on the capillary tube. The transmit signal was generated by an arbitrary wave generator (8026, Tabor Electronics Ltd., Tel Hannan, Israel) and amplified with a power amplifier (150A100B Amplifier Research, Limerick, Ireland). The diluted bubble solution was injected into the capillary. Bubbles with a diameter ranging between 3 and 10 µm were insonified by driving frequencies from 0.5 to 3.9 MHz with frequency steps of 200 kHz and at an acoustic pressure of 50 kPa and 100 kPa. A 10 cycle tapered burst at an acoustithe first and last 2 cycles. The recorded images were magnified using a 60×water-immersed objective and a 2× magnifier. The dynamics of the bubbles was captured by the Brandaris 128 ultra high speed camera at a frame rate of 15 million frames per second. For each movie the diameter of the microbubble as a function of time (d-t curve) was analyzed (Fig. 2) and the maximum amplitude of radial excursions of each drive frequency at a constant pressure was selected to construct a resonance curve for each individual microbubble.

C. *Spectroscopy of pressure sweeping experiment*

For pressure sweeping measurements the capillary tube was replaced by an OptiCell chamber (NUNC™, Thermo Fisher Scientific, Roskilde, Denmark). The applied acoustic pressures were as follows: 5 to 50 kPa with pressure steps of 5 kPa, then 75 kPa and finally 100 kPa. Frequencies were varied between 0.5 to 3.9 MHz with frequency step of 200 kHz.

D. *Fluorescence imaging*

The stability of the liposomes attachment was assessed by comparing the fluorescence images before and after insonation showing the bodipy-labeled liposomes. Fluorescence imaging light source is a 460 nm wavelength laser (Cohlibri, Lightline, Santa Clara, CA) and the receiver is a CCD camera (LM165, Lumenera, Ottawa, CA).

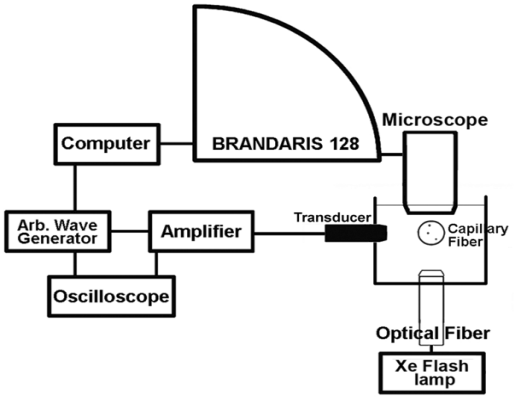

Figure 1. Schematic setup for frequency scanning experiments.

This work was supported by Sonodrugs Project (NMP-4-LA-2008-213706) with financial support from the European Union.

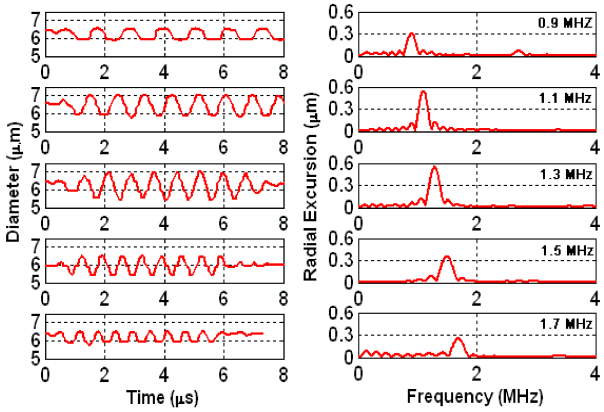

Figure 2. Selected d-t curves and corresponding power spectra of an LPS bubble with a diameter of 6.4 µm.

III. RESULTS

A. *Shell elasticity*

A uniform shell elasticity for bubble of various sizes is estimated from the fitting of the resonance frequencies measured experimentally versus the bubbles diameter (Fig. 3) to a linearized Marmottant model as described by van der Meer *et al.* (2007).

$$f_0 = \frac{1}{2\pi}\sqrt{\frac{1}{\rho R_0^2}\left[3\gamma P_0 + \frac{2(3\gamma-1)\sigma_\omega}{R_0} + \frac{4\chi}{R_0}\right]} \quad (1)$$

f_0 is the eigenfrequency of the microbubble; P_0 is the ambient pressure; R_0 is the equilibrium radius; $\rho=10^3$ kg/m^3 is the density of water; $\gamma=1$ is the polytropic exponent of an isothermal vibration; σ_ω is the surface tension of water and χ is the shell elasticity. At 50 kPa, the estimated elastic contribution to the resonance frequency of the bare bubbles is found for χ = 0.19±0.1 N/m, which is very close to the value found for LPS bubbles, χ = 0.17±0.1 N/m.

B. *Shell viscosity*

The shell viscosity (κ_s) is estimated from the total damping coefficient (δ_{tot}) as follows:

$$\delta_{tot} = \frac{\omega_0 R_0}{c} + \frac{4\mu}{R_0^2\rho\omega_0} + \frac{4\kappa_s}{R_0^3\rho\omega_0} \quad (2)$$

δ_{tot} is the sum of the contributions of acoustic re-radiation, viscous damping of the liquid and the shell viscous damping coefficient respectively; $c=1.5\times10^3$ m/s is the speed of sound in water; $\mu=2\times10^{-3}$ Pa.s is the liquid viscosity and is slightly increased to account for the contribution of thermal damping. The estimated shell viscosity of the bare bubbles and LPS bubbles as a function of the bubbles diameter is depicted in Fig. 4. On average, the shell viscosity of the LPS bubbles (2.5×10^{-8} kg/s) is nearly 2 times that of the bare bubbles (1.4×10^{-8} kg/s).

C. *Pressure dependent Resonance*

Fig. 5 shows the experimentally obtained amplitude of oscillations of a bare bubble and an LPS bubble (with a diameter of 6.6 µm) as a function of the applied acoustic pressure and driving frequency. Each plot contains 12 resonance curves which are derived from a total of 204 D-t curves of the very same bubble [12]. It was observed that the resonance frequency of bare bubbles and LPS bubbles decreases with increasing acoustic pressure. Moreover, at the same acoustic pressure, the bare bubbles have higher amplitude of oscillation than the LPS bubbles.

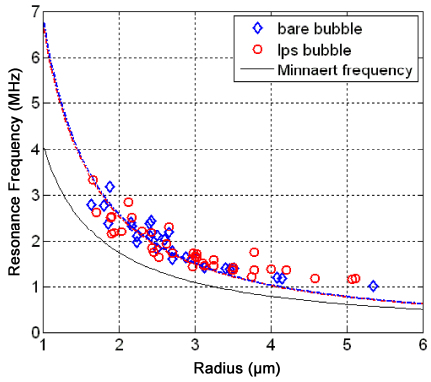

Figure 3. The resonance frequency as a function of bubble radius at an acoustic pressure of 50 kPa.

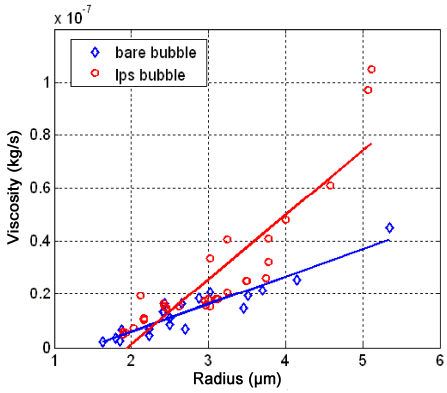

Figure 4. Viscosity as a function of bubbles radius.

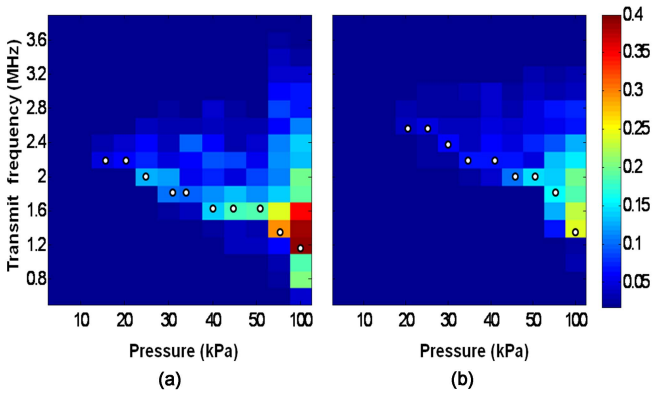

Figure 5. Amplitude of oscillation as a function of driving frequency and pressure for a) a bare bubble and b) an LPS bubble with 6.6 µm diameter.

Fig. 5 also shows that the threshold pressure for the initiation of bubble oscillations is higher for the LPS bubble than for the bare bubble. This higher threshold pressure for the LPS bubble was confirmed in a specific study while the acoustic pressure was varied.

D. *Expansion-only behavior*

Among the 73 LPS bubbles and 41 bare bubbles investigated in this study, 69% of the LPS bubbles showed expansion-only (EO) behavior, while among bare bubbles, only 13% showed EO behavior. A typical example is shown in Fig. 6. It indicates strongly hindered bubble compression. A scan of the pressure showed that LPS bubbles exhibit EO behavior at lower acoustic pressures compared to the bare bubbles. Nearly 50% of the investigated LPS bubbles show EO behavior below 30 kPa, see Table I.

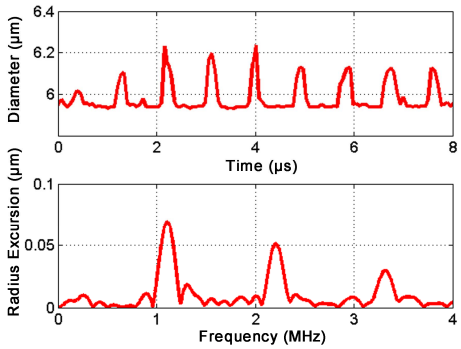

Figure 6. D-t curve of the oscillations of an LPS bubble (5.9 µm diameter) exhibiting the expansion-only behavior.

TABLE I. Pressure dependence of EO behavior

Pressure (kPa)	*EO occurrence of bare bubbles (%)*	*EO occurrence of LPS bubbles (%)*
10	0	5.7
20	0	18.6
30	14.3	22.9
40	21.4	18.6
50	28.6	15.7
75	28.6	11.4
100	7.1	7.1

E. *Liposome attachment*

Fig. 7 shows the fluorescent images of the liposome attachment before and after 204 consecutive insonations with ultrasound pulses. The frequency ranged from 0.6 MHz to 3.8 MHz and the acoustic pressures ranged from 5 kPa to 100 kPa, similar to settings applied during the pressure sweeping experiments. Images clearly show the presence of a stable liposome layer attached to the microbubble shell.

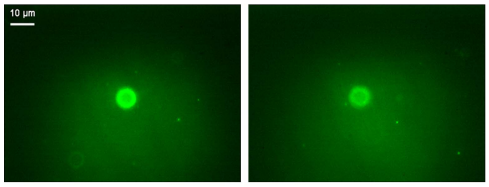

Figure 7. Laser-induced fluorescence imaging of bodipy labeled LPS bubbles a) before and b) after insonation.

IV. DISSCUSSION

In this study, we use bare bubbles as a reference, and investigated the shell properties and the ultrasonic behavior of LPS bubbles as a function of the frequency and the acoustica pressure. Compared with the bare bubbles, the shell of LPS bubbles have the same elasticity, but higher viscosity, especially for bubbles larger than 6 µm. Thresholding behavior was observed for both populations of bubbles, and a higher pressure threshold value was found for LPS bubbles. In addition, a characteristic expansion-only behavior was found for LPS bubbles, with half of them occurred at low acoustic pressures (≤30 kPa).

We ascribe the increase of shell viscosity to the surface morphology of LPS bubbles, where crosslinking of the liposome layer produce these effects. It was reported that for polymer materials, a low crosslink density between polymer chains raise the viscosity of the material, while a high crosslink density increases the strengths and rigidity of the material [13]. We propose that the comparatively low crosslink density on the LPS bubbles causes the energy loss during bubble oscillations, thus leading to higher "internal friction". The damping of LPS bubble oscillations due to a higher viscosity in turn leads to a larger pressure threshold. On the other hand, packing together of the liposomes during compression prevents the bubble from contracting, leading to expansion-only behavior at low acoustic pressures [14].

The driving parameters used in this study will facilitate future preclinical studies and clinical applications using LPS bubbles. In a further step, the comprehensive acoustical characterization of LPS bubbles provides a better understanding of the correlation between bubble morphology, shell properties and ultrasonic behavior of LPS bubbles. This would provide us with instructions on the preparation of the LPS bubbles, or similar drug loaded microbubbles, for their applications in ultrasound triggered drug delivery system. Larger LPS bubbles are preferable for the purpose of higher drug loading capacity and for a safer drug transportation, although these bubbles suffer from a higher damping and a higher pressure threshold. By manipulating the liposome loading and its local distribution on the microbubble shell, the acoustical response of LPS bubbles can be well-controlled. The highly nonlinear response of LPS bubbles caused by expansion-only behavior under low acoustic pressures indicates its great potential in therapeutic applications such as contrast imaging and drug delivery under lower Mechanical Index (MI), due to its beneficial effect to introduce local flow phenomena, such as acoustic microstreaming around microbubbles with minimized risk of cell damaging or microbubble destruction.

ACKNOWLEDGMENT

We would like to thank Frits Mastik, Robert Beurskens and Michiel Manten for their technical support. We also thank Guillaume Renaud, Marlies Overvelde and Klazina Kooiman for valuable discussions.

REFERENCES

[1] K. Ferrara, R. Pollard, and M. Borden, "Ultrasound microbubble contrast agents: fundamentals and application to gene and drug delivery," *Annu Rev Biomed Eng,* vol. 9, pp. 415-47, 2007.

[2] C. M. Newman and T. Bettinger, "Gene therapy progress and prospects: ultrasound for gene transfer," *Gene Ther,* vol. 14, pp. 465-75, 2007.

[3] A. Kheirolomoom, P. A. Dayton, A. F. Lum, E. Little, E. E. Paoli, H. Zheng, and K. W. Ferrara, "Acoustically-active microbubbles conjugated to liposomes: characterization of a proposed drug delivery vehicle," *J Control Release,* vol. 118, pp. 275-84, 2007.

[4] B. Geers, I. Lentacker, N. N. Sanders, J. Demeester, S. Meairs, and S. C. De Smedt, "Self-assembled liposome-loaded microbubbles: The missing link for safe and efficient ultrasound triggered drug-delivery," *J Control Release,* vol. 152, pp. 249-56, 2011.

[5] N. de Jong, R. Cornet, and C. T. Lancée, "Higher harmonics of vibrating gas-filled microspheres. Part one: simulations," *Ultrasonics,* vol. 32, pp. 447-453, 1994.

[6] C. C. Church, "THE EFFECTS OF AN ELASTIC SOLID-SURFACE LAYER ON THE RADIAL PULSATIONS OF GAS-BUBBLES," *Journal of the Acoustical Society of America,* vol. 97, pp. 1510-1521, 1995.

[7] P. Marmottant, S. van der Meer, M. Emmer, M. Versluis, N. de Jong, S. Hilgenfeldt, and D. Lohse, "A model for large amplitude oscillations of coated bubbles accounting for buckling and rupture," *Journal of the Acoustical Society of America,* vol. 118, pp. 3499-3505, 2005.

[8] S. Meer van der, B. Dollet, C. T. Chin, A. Bouakaz, M. Voormolen, N. Jong de, M. Versluis, and D. Lohse, "Microbubble spectroscopy of ultrasound contrast agents (A)," *Journal of the Acoustical Society of America,* vol. 120, p. 3327, 2006.

[9] M. Emmer, A. van Wamel, D. E. Goertz, and N. de Jong, "The onset of microbubble vibration," *Ultrasound Med Biol,* vol. 33, pp. 941-9, 2007.

[10] N. de Jong, M. Emmer, C. T. Chin, A. Bouakaz, F. Mastik, D. Lohse, and M. Versluis, ""Compression-only" behavior of phospholipid-coated contrast bubbles," *Ultrasound Med Biol,* vol. 33, pp. 653-6, 2007.

[11] M. Overvelde, V. Garbin, J. Sijl, B. Dollet, N. de Jong, D. Lohse, and M. Versluis, "Nonlinear shell behavior of phospholipid-coated microbubbles," *Ultrasound Med Biol,* vol. 36, pp. 2080-92, 2010.

[12] M. Overvelde, V. Garbin, J. Sijl, B. Dollet, N. de Jong, D. Lohse, and M. Versluis, "Nonlinear Shell Behavior of Phospholipid-Coated Microbubbles," *Ultrasound in Medicine & Biology,* vol. 36, pp. 2080-2092, 2010.

[13] C. M. Tierney, M. G. Haugh, J. Liedl, F. Mulcahy, B. Hayes, and F. J. O'Brien, "The effects of collagen concentration and crosslink density on the biological, structural and mechanical properties of collagen-GAG scaffolds for bone tissue engineering," *J Mech Behav Biomed Mater,* vol. 2, pp. 202-9, 2009.

[14] E. Stride, K. Pancholi, M. J. Edirisinghe, and S. Samarasinghe, "Increasing the nonlinear character of microbubble oscillations at low acoustic pressures," *J R Soc Interface,* vol. 5, pp. 807-11, 2008.